Special Issue for ICASGE'19

Monitoring Crack Propagation in R. C. Coupled Shear Walls Supported on Two Columns

Amir A. EL-Fadeel, Naser F. EL-Shafey, Heba M. Issa

MONITORING CRACK PROPAGATION IN R. C. COUPLED SHEAR WALLS SUPPORTED ON TWO COLUMNS

Amir A. EL-Fadeel [1], Naser F. EL-Shafey [2], Heba M. Issa [3]

[1]*Assistant lecturer, Misr Higher Institute for Engineering and Technology, Mansoura, Egypt*
E-mail: amirabdelfadeel@gmail.com
[2]*Associate Professor, Faculty of Engineering, Cairo University, Egypt*
E-mail: elshafey.nasser@gmail.com
[3]*Assistant Professor, R. C. Institute Housing & Building National Research Center, Egypt*
E-mail: heba.m.issa@gmail.com

ABSTRACT:

Many efforts have been made to monitor the cracking behaviour in RC structures. The objective of this paper is to present the results of a theoretical study aimed at monitoring the behavior of coupled shear walls supported on two columns in elastic and post elastic stage, also drift at each story, stress and strain for both concrete and steel reinforcement, and crack propagation. Consequently, a case study was assumed, where three-dimensional, non-linear finite element analysis was carried out for eighteen samples taking into consideration cracking and crushing of concrete, as well as yielding of rebars.
The results were reported as the effect of characteristic strength, stiffness ratio between columns and walls, on the ultimate horizontal load capacity and the ductility of the entire system. The results demonstrate that stiffness ratio between shear walls and supporting columns is more crucial on the response of the coupled system rather than characteristic strength, and the position of first flexural and shear cracks are predominated by transfer beam stiffness.

Keywords: Coupled shear walls supported on columns; Earthquake; Non-linear finite analysis, Cracks in shear walls.

INTRODUCTION:

Coupled shear walls supported on columns can be used at ground floors, because of parking requirements. These configurations of coupled shear walls decrease the lateral stiffness and result in stress concentration at the connections between the shear walls and the supporting columns. This system contains shear walls which are dominated by flexural behaviour, and frames which are dominated by its shear deformation. Therefore, the whole behaviour of this system is a hybrid of flexural and shear deformation.

Morgan [1] studied seven stories coupled shear walls supported on columns under vertical loads only. This study included material linearity and non-linearity of two dimensional reinforced concrete structures under the action of monotonically increased loads. This study based on finite element analysis by using of (NARCS10) program. The finite element analysis by (NARCS10) program included iso-parametric quadrilateral element, and steel reinforcement was modeled using two nodes discrete bar element as well as smeared steel element. It concludes that transfer beam must have a height not less than 20% of the clear span of the lower wide floor, increasing or decreasing the amount of main steel of this type of structures has inconsequential effect on the ultimate load of the wall. This means that, the failure of the wall is

mainly controlled by the ultimate compressive strength of concrete, and the use of 4, 5 and 6 nodes quadrilateral elements gives reasonable accuracy for the results.

Khaled [2] studied the same system of Morgan [1] using a finite element program (ANSYS). In addition to pushover analysis, and addressing the effect of stiffness variation of columns, coupling beams, transfer beams and link beams. Moreover, scrutinized the load path dependence for gravitational and pushover combinations. It concludes that the stress concentration pattern significantly differs depending on the type of loading. Geometric discontinuity regions capture the highest damage evolution rate. For example, under gravitational loading stress concentration takes place at the column-wall junction and also in the transfer and the link beams. On the other hand, for lateral loading the highest tensile stresses occur at the column-wall junction of the loaded side and in coupling beams. Redistribution of stresses is evident through the course of loading with emphasis to the relative column to coupled shear wall stiffness. In turn, the position of the maximum bending stresses shifts from the base upwards with the progress of loading. The same system of Khaled [2], as an example, used to validate the use of "ANSYS (14)" [3] program in the present study. Eventually, the results obtained from the analysis are nearly the same results of Khaled's model.

The main objectives of present work are to provide the several parameters required to have a better understanding of the behavior of the coupled shear walls supported on columns under quasi-static loading. The main objectives can be summarizing as the following:

1- Understanding the behavior of the coupled system taking into consideration the effect of material nonlinearity in vertical loading besides static pushover analysis.

2- Analyzing the response of the coupled system on the ultimate horizontal load capacity, the ductility of the whole system under the effect of characteristic strength, stiffness ratio between columns and walls.

CASE STYDY

Geometry Dimensions

Plan area (20×30 m), Shear wall cross-section (0.5×4 m), Columns cross-section(0.5×1.5 m), Connecting beams cross-section(0.5×0.6 m), Transfer beam cross-section(0.5×1.5 m). The plane and elevation of the case study are shown in Figure (1).
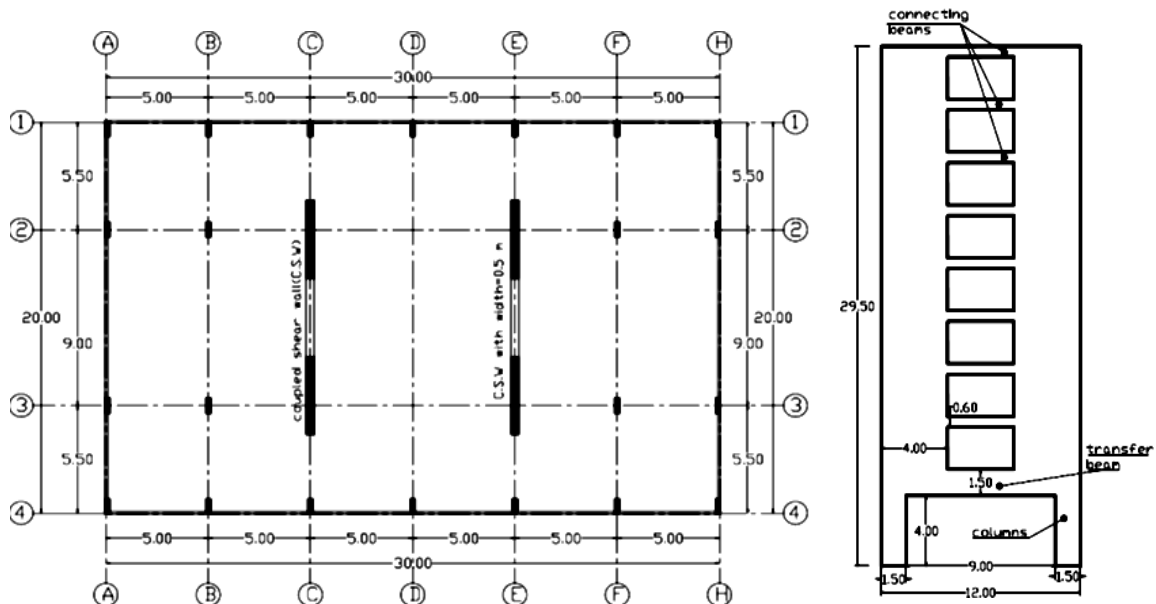
Figure 1: Plan and Elevation of the coupled shear walls supported on columns

Vertical and Horizontal Loads

Factored vertical loads are calculated due to weight of walls, coupling beams, columns, in addition to loads from the weight of slabs, where: live load=4 kN/m^2, flooring load =1.5 kN/m^2, weight of brick walls=1.5 kN/m^2, thickness of slabs= 220 mm. Additionally, distributed vertical loads/story =100 kN/m. Horizontal loads are calculated by the simplified response spectrum analysis using "ECP-203" [4], in which horizontal loads are distributed by the inverse of triangle with a maximum value, 500 KN, at the top floor level. Vertical and Horizontal loads cab be calculated as shown in Appendix (A).

Definition of Ductility

The ductility definition is the capability of the material/member to endure deformation beyond the elastic limit. To evaluate the ductility, the deformation may be strain, curvature, displacement or rotation. According to "Pam et al.," [6] it is better to express the ductility in terms of a dimensionless ductility factor (µ) as shown in equation (1).

$$\mu = \left[\frac{\Delta max}{\Delta y}\right] \tag{1}$$

Where: (Δ_{max}) is the maximum deformation, at which the crushing of concrete for any structural member occurs. And (Δ_y) is the yielding deformation, at which the reinforcement for any structural element yields.

Main Parameters

The main parameters taken into consideration are listed below in Table (1).

Table 1: Main parameters of the case study.

Sample Number	Main parameters					
	f'_c(MPa)	Reinforcement ratio (µ%)				$\left[\dfrac{t\_column}{t\_wall}\right]\%$
		column	Transfer beam	wall	Connecting beam	
1	35	0.8%	0.68%	0.62%	0.92%	37.5%
2	35	0.8%	6.5%	0.62%	0.92%	37.5%
3	35	3.7%	6.5%	1.17%	3.9%	37.5%
4	35	0.8%	0.68%	0.62%	0.92%	51.25%
5	35	0.8%	6.5%	0.62%	0.92%	51.25%
6	35	3.7%	6.5%	1.17%	3.9%	51.25%
7	45	0.8%	0.68%	0.62%	0.92%	37.5%
8	45	0.8%	6.5%	0.62%	0.92%	37.5%
9	45	3.7%	6.5%	1.17%	3.9%	37.5%
10	45	0.8%	0.68%	0.62%	0.92%	51.25%
11	45	0.8%	6.5%	0.62%	0.92%	51.25%
12	45	3.7%	6.5%	1.17%	3.9%	51.25%
13	60	0.8%	0.68%	0.62%	0.92%	37.5%
14	60	0.8%	6.5%	0.62%	0.92%	37.5%
15	60	3.7%	6.5%	1.17%	3.9%	37.5%
16	60	0.8%	0.68%	0.62%	0.92%	51.25%
17	60	0.8%	6.5%	0.62%	0.92%	51.25%
18	60	3.7%	6.5%	1.17%	3.9%	51.25%

FINITE ELEMNET ANALYSIS

The finite element analysis using "ANSYS (14)" [3] package can be used to closely forecast the behavior of the coupled system which subjected to in-plane forces. The load-deflection behavior, crack propagation, first crack load, failure load, and failure mode can be predicted using the finite element method with an accuracy that is acceptable for engineering purposes. Furthermore, the program accounts for: (1) material non-linearity of both concrete and steel, (2) biaxial failure surface of concrete, (3) nonlinear stress-strain curve of steel and (4) concrete cracking and crushing.

Material properties

Concrete

Concrete in compression: the idealized stress strain curve as in ECP-203 [4] can be used for representing the actual behavior of concrete in compression. It consists of a parabola up to a strain of 0.002 and straight horizontal line up to a strain of 0.003.

Concrete in Tension: the tensile strength of concrete is very low and it might be generally about 10% of its compressive strength for normal concrete, but the tensile strength of high strength concrete can be calculated from equation (2) according to "Martinez et al.,"[7]. In this study, concrete is assumed to behave as a linear elastic-brittle material in tension, and this is an essential factor causing the nonlinear behavior. Cracks are assumed to form in planes perpendicular to the direction of maximum principal tensile stress as soon as this reaches the specified concrete tensile strength.

$$f'_{sp} = 0.59\sqrt{f'_c} \quad \text{MPa} \tag{2}$$

The "SOLID65" element: A concrete 3D- solid element was used to model the behavior of concrete with reinforcing bars which requires linear isotropic and multi-linear isotropic material properties to properly model for concrete. The multi-linear isotropic material uses the Von-Misses failure criterion along with the "Willam and Warnke," [8] model to define the failure of the concrete. "EX" is the initial tangent modulus of elasticity of the concrete (E_c) and "PRXY" is the Poisson's ratio (v). The young's modulus for normal concrete (concrete with compressive strength less than (41 MPa) approximately) is depended on the following equation (3), and the young's modulus for high strength concrete (concrete with compressive strength in excess (41 MPa) approximately) is depended on the following equation (4) defined by "Martinez, S., Nilson, Ah., and Slate, F.O.," [7] .

$$E_c = 4700\sqrt{f'_c} \quad (MPa) \tag{3}$$

$$E_c = 3320\sqrt{f'_c} + 6900 \quad (MPa) \qquad (for\ 21\ MPa < f'_c < 83\ MPa) \tag{4}$$

Where a value of, f'_c equal to a cylinder compressive strength in (MPa) units, and Poisson's ratio is assumed to be 0.2 for concrete. The uniaxial compressive stress-strain relationship for the concrete model is obtained using the following equations (5, 6, 7) to calculate the multi-linear isotropic stress-strain curve for the concrete in compression "Wight and Macgregor," [9] and this equation will be used in the present study:

$$f = \frac{E_c \varepsilon_c}{1 + \left(\frac{\varepsilon_c}{\varepsilon_o}\right)^2} \tag{5}$$

$$\varepsilon_o = \frac{2f'_c}{E_c} \tag{6}$$

$$E_c = \frac{f}{\varepsilon_c} \tag{7}$$

Where f is the stress at any strain ε_c and ε_o is the strain at the cylinder compressive strength f_c'. the multi-linear isotropic stress-strain curve, demands the first point of the curve to be entered by the user. It must satisfy Hooke's Law. The multi-linear curve is used to help for the convergence of the nonlinear solution algorithm as shown in figure (3).

The model that capable of predicting failure of concrete material is shown in Figure (2). Both cracking and crushing failure modes are taken into consideration. The two input strength parameters i.e., ultimate tensile and compressive strengths are demanded to define a failure surface of the concrete. Consequently, a criterion for failure of the concrete due multi-axial stress state can be calculated "Willam and Warnke" [8].
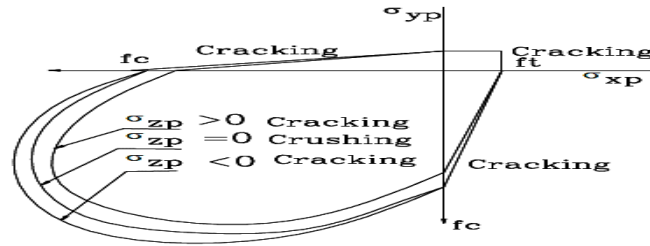
Figure 2: Failure surface of the concrete.

In concrete element, cracking occurs when the principal tensile stress in any directions lies outside the failure surface. After cracking, the young's modulus of concrete element is set to zero in the direction parallel to the principal tensile stress direction. Crushing takes place when all principal stresses are compressive and lie outside the failure surface. Thereafter, the young's modulus is set to zero in all directions, and the element effectively disappears.

For the implementation of the "Willam and Warnke" [8], material model in "ANSYS (14)" requires defining nine constants as shown in Table (2).

Steel reinforcement

The "Link 8-3D" element is used to model steel reinforcement. This element is a uniaxial tension-compression element. The mechanical properties of steel are well-known and understood. Steel is homogeneous and has usually the same yield strength in tension and compression. In the present study reinforcing steel is modeled as a bilinear elasto-plastic material using the idealized stress-strain curve as shown in figure (4).
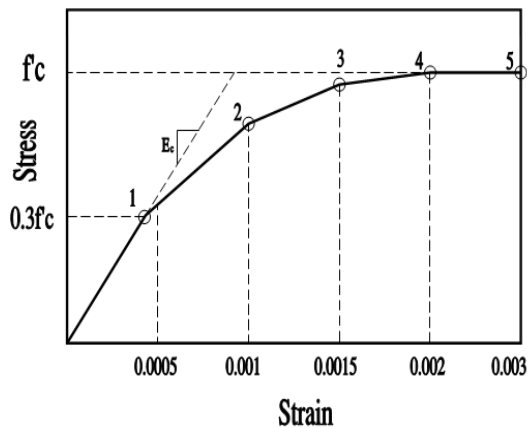
Fig.3: Idealized stress-strain curve for concrete in compression
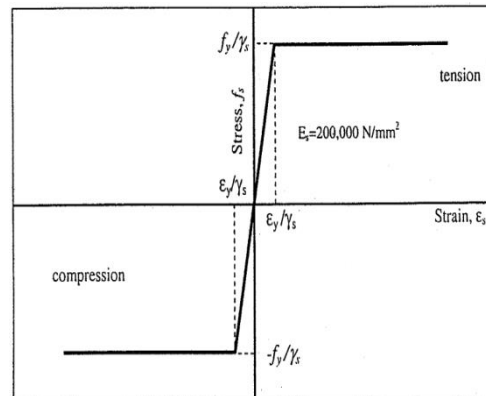
Fig.4: Idealized stress-strain curve for steel reinforcement

Material Modeling

Table 2: Material models for "SOLID65, LINK8 Element".

Material Model No.	Element Type	Material Properties	
1	SOLID65	**Linear Isotropic**	
		Elasticity Modulus, EX, is equal to $(\frac{f_1}{\varepsilon_1})$ at point (1) at the curve.	
		Poisson's Ratio, PRXY, is equal to 0.20	
		Multi-linear Isotropic	
		Five coordinates are needed to represent the stress-strain curve for concrete, Figure (3).	
		Concrete	
		Open Shear Transfer Coeff.	0.2
		Closed Shear Transfer Coeff.	0.9
		Uniaxial Cracking Stress (Modules of rupture)	The concrete tensile strength f_t is typically 8% - 15% of the compressive strength and taken equal to 10% for normal concrete, and according to equation (2).
		Uniaxial Crushing Stress	The crushing stress value is taken from the stress-strain curve.
		Biaxial Crushing Stress	0
		Hydrostatic Pressure	0
		Hydro Biaxial Crush Stress	0
		Hydro Uniaxial Crush Stress	0
		Tensile Crack Factor	0
2	LINK8	**Linear Isotropic**	
		Elasticity Models, EX, is equal to $2 \times 10^5 \text{MPa}$	
		Poisson's Ratio PRXY, is equal to 0.30	
		Bilinear Isotropic	
		Yield Stresses follow the design material properties used for the experimental investigation.	
		Tangent Modulus is taken equal to Yield Stress.	

Modeling of coupled shear walls supported on columns by ANSYS program

Modeling of the coupled shear walls system is carried out where the node points of the solid elements coincide with the actual reinforcement locations as shown in figure (5). Moreover, the shape of proposed reinforcement is illustrated in the same aforementioned figure. The proposed reinforcing steel of the coupling beams, which are considered in the present study as a slender beams (span to depth ratio is more than nearly 2.5), is assumed to be in the conventional form of reinforcement without taking into consideration the diagonal

reinforcement. This assumption may be considered to tackle the issue of the accurate placement of the inclined reinforcement during construction, however, the diagonally reinforced slender coupling beams performed significantly better than conventionally slender coupling beams, "Zhou, J.," [15].   .
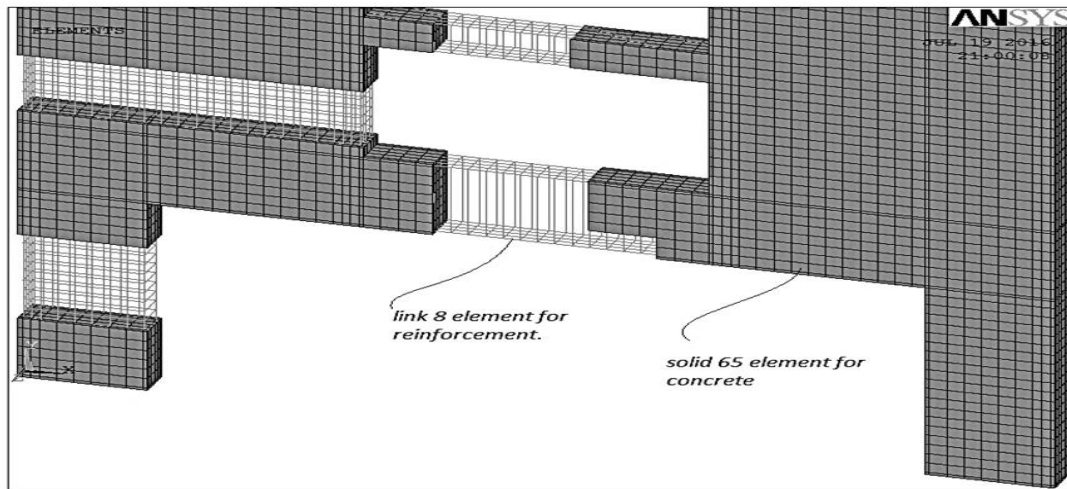
Figure 5: Modeling of the coupled shear walls system using ANSYS

PUSHOVER ANALYSIS AND RESULTS

Lateral loads represent one of the major concerns in high-rise buildings. Figure (9) shows the variation of top drift for all samples at different increments of loading. Apparently, the trend is nearly linear along the height at low load levels. However, at higher load increments, the drift at higher stories considerably differs and the trend tends to be non-linear.

To illustrate the steps of loading as well as understanding the behavior of the coupled system, sample (12) can be taken as an example. At the beginning of loading, the structure is deformed until the first flexural cracks are taken place at load 137.5 kN, therefore this load is considered as the first crack load (Pcr). At load 237.5 kN, first shear cracks are observed, therefore this load is considered as the first shear crack load (Pv), as well as increasing in flexural cracks propagation. By increasing the loading rate until load 575 kN which is considered yielding load (p_y) because of the beginning of yielding for stirrups of transfer beam. The value of drift at the top point is found equal to 57.99 mm ($\triangle_y$), as well as forming of the first plastic hinge at connecting beam no.4 which is counted from the top floor as shown in figure (7-a) - According to "Coull, A." [11], it is assumed that the plastic hinge forms at the middle third of the height of the coupled system. Because of the beginning of yielding for stirrups of transfer beam, the elastic range is considered ended and the post-elastic range is begun.

 By helping the vector mode option of "ANSYS (14)" [1], it is observed that the regions of stress concentrations for the three principles stress at failure load as shown in figure (6). These principle stresses are defined by "Timoshenko,S., Goodier,J.N.," [12]. The first principle stress represents a maximum value (tension zone), and the third principle stress represents a minimum value (crushing zones). It is also found that further increasing of the loading rate would lead to the second plastic hinge at load 650 kN, which is considered the failure load (P_u) because of the crushing of concrete for the supporting columns as shown in figure (7-b). At this load, it is also spotted the crushing of concrete for transfer beam at the junction between connecting beams and the shear walls. In addition, the maximum drift (Δ_{max}) is founded equal to 71.46 mm as shown in figure (8).

The main results for all samples are summarized in two main groups as shown in Tables (3) and (4): Group one includes samples number (1, 2, 3, 7, 8, 9, 13, 14, and 15) with stiffness ratio 37.5% between columns and walls. Group two includes samples number (4, 5, 6, 10, 11, 12, 16, 17, and 18) with stiffness ratio 51.25%.
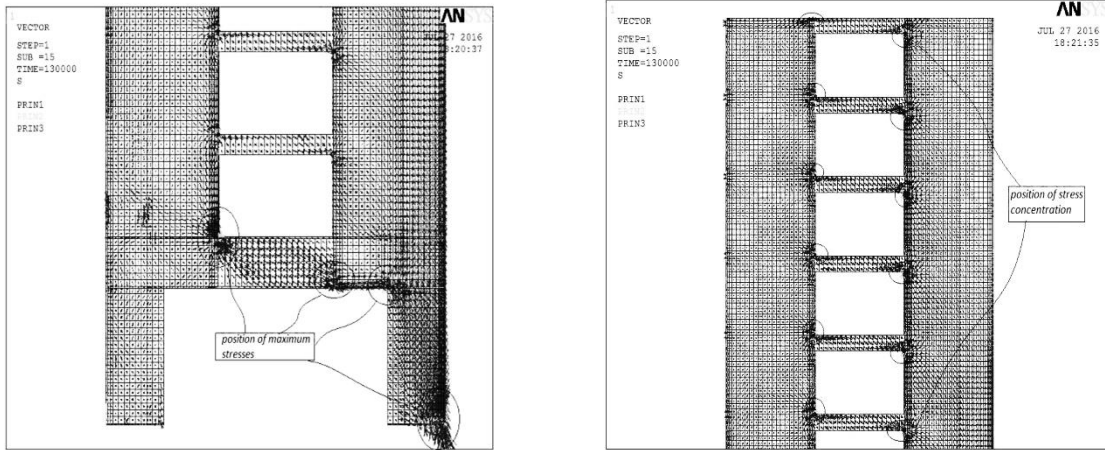
Figure 6: Principles stresses at failure load for sample (12).
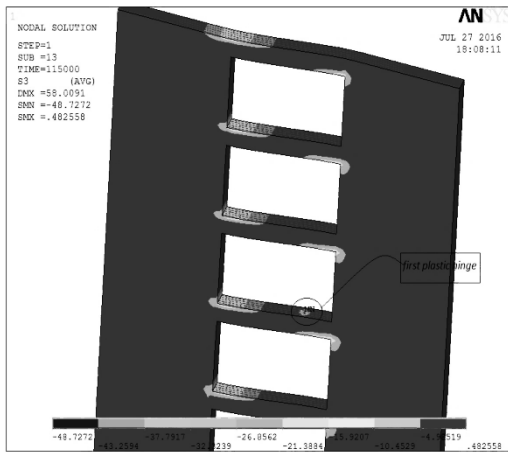
Fig.7-a: 1ˢᵗ plastic hinge for sample (12).
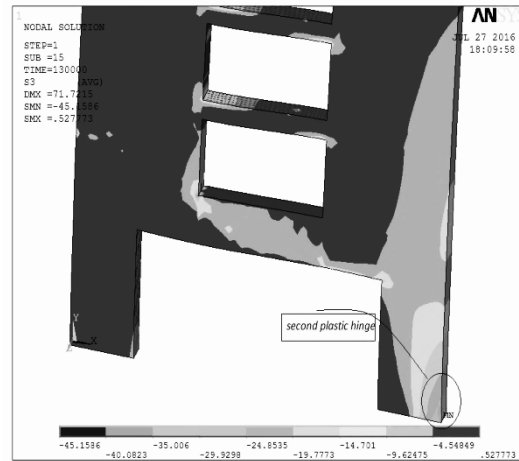
Fig.7-b: 2ⁿᵈ plastic hinge for sample (12).
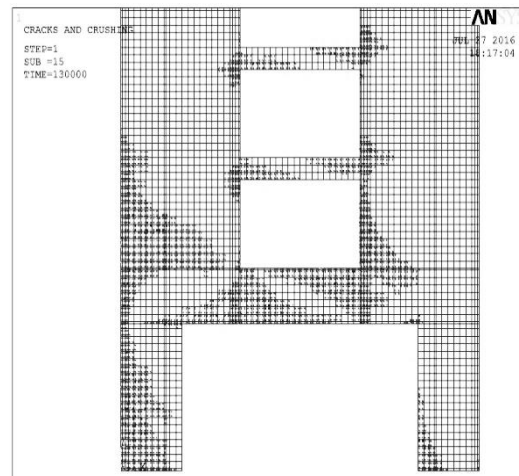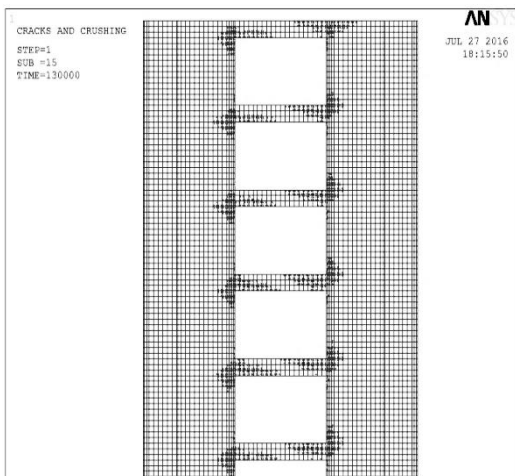
Figure 8: crack pattern at failure load for sample (12).
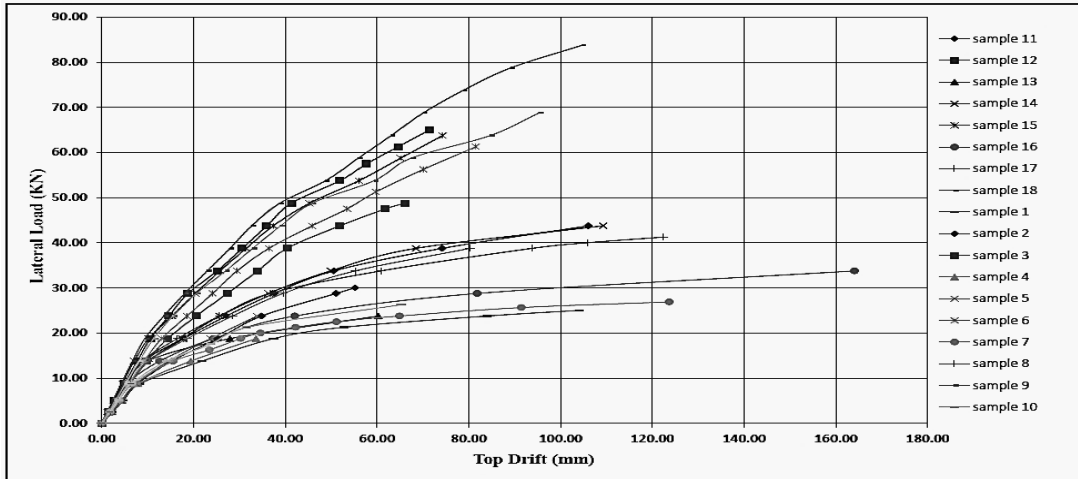
Figure 9: The variation of top drift for all samples at different increments of loading

Table (3) Results of Group one

	Sample Number	Pcr (ton)	Pv (ton)	Py (ton)	Pu (ton)	Yielding drift (mm)	Max. Drift (mm)	Fcu (Mpa)	Ductility (%)
group one	1	8.75	13.75	13.75	25	21.93	104.22	35	4.75
	2	8.75	13.75	23.75	30	35.09	55.45	35	1.58
	3	13.75	18.75	38.75	48.75	40.59	66.26	35	1.63
	7	8.75	13.75	13.75	26.88	15.69	124.03	45	7.91
	8	8.75	18.75	23.75	38.75	28.68	80.49	45	2.81
	9	13.75	23.75	33.75	58.75	27.16	67.67	45	2.49
	13	8.75	13.75	18.75	23.75	28.04	60.37	60	2.15
	14	8.75	18.75	28.75	43.75	36.49	109.5	60	3.00
	15	13.75	23.75	33.75	63.75	25.89	74.28	60	2.87

Table (4) Results of Group two

	Sample Number	Pcr (ton)	Pv (ton)	Py (ton)	Pu (ton)	Yielding drift (mm)	Maxim. Drift (mm)	Fcu (Mpa)	Ductility ratio (%)
group two	4	8.75	13.75	13.75	18.75	19.52	33.64	35	1.72
	5	8.75	13.75	23.75	23.75	34.81	34.81	35	1.00
	6	13.75	23.75	51.25	61.25	60.02	81.51	35	1.36
	10	8.75	13.75	13.75	26.25	14.22	65.28	45	4.59
	11	8.75	18.75	23.75	43.75	27.33	106.05	45	3.88
	12	13.75	23.75	57.5	65	57.99	71.46	45	1.23
	16	8.75	13.75	18.75	33.75	24.31	164.06	60	6.75
	17	8.75	18.75	28.75	41.25	36.84	122.45	60	3.32
	18	13.75	23.75	73.75	83.75	78.99	104.66	60	1.32

Effect of characteristic strength (fcu) on ultimate horizontal load capacity, load of first shear cracks, load of first flexural cracks, and ductility can be illustrated by figures 10, 11, 12, and 13 respectively. Samples are assembled through a table beneath every single bar-chart according to table (5).

Table (5) Samples assembly for the case of effect (f_{cu})

	a	b	c	d	e	f
fcu=30	1	2	3	4	5	6
fcu=45	7	8	9	10	11	12
fcu=60	13	14	15	16	17	18

Effect of (fcu) on (pu)

	a	b	c	d	e	f
35	25	30	48.75	18.75	23.75	61.25
45	26.88	38.75	58.75	26.25	43.75	65
60	23.75	43.75	63.75	33.75	41.25	83.75
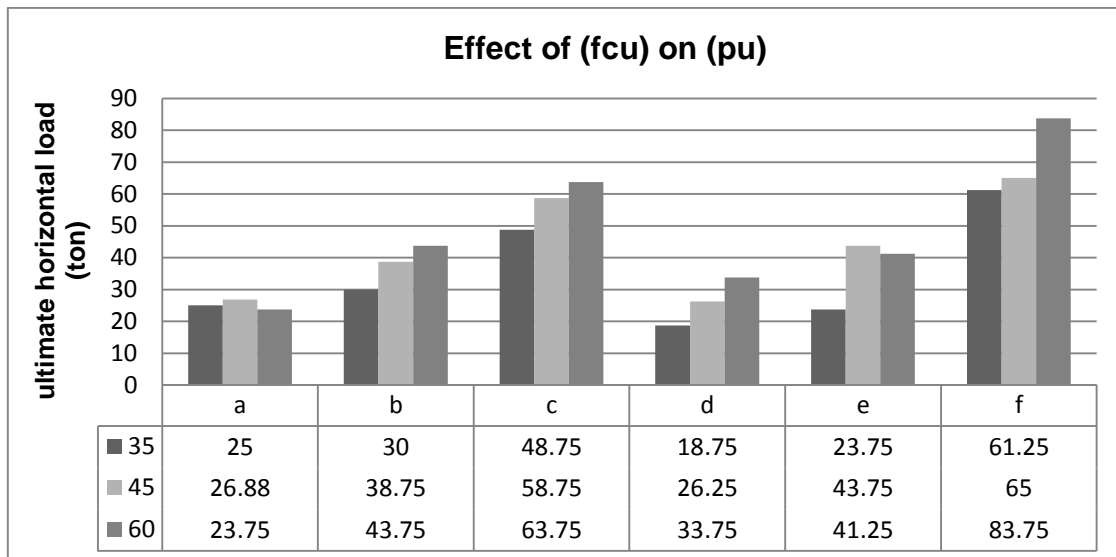
Figure 10: Effect of characteristic strength (f_{cu}) on ultimate horizontal load (p_u)

Effect of (fcu) on (pv)

	a	b	c	d	e	f
35	13.75	13.75	18.75	13.75	13.75	23.75
45	13.75	18.75	23.75	13.75	18.75	23.75
60	13.75	18.75	23.75	13.75	18.75	23.75
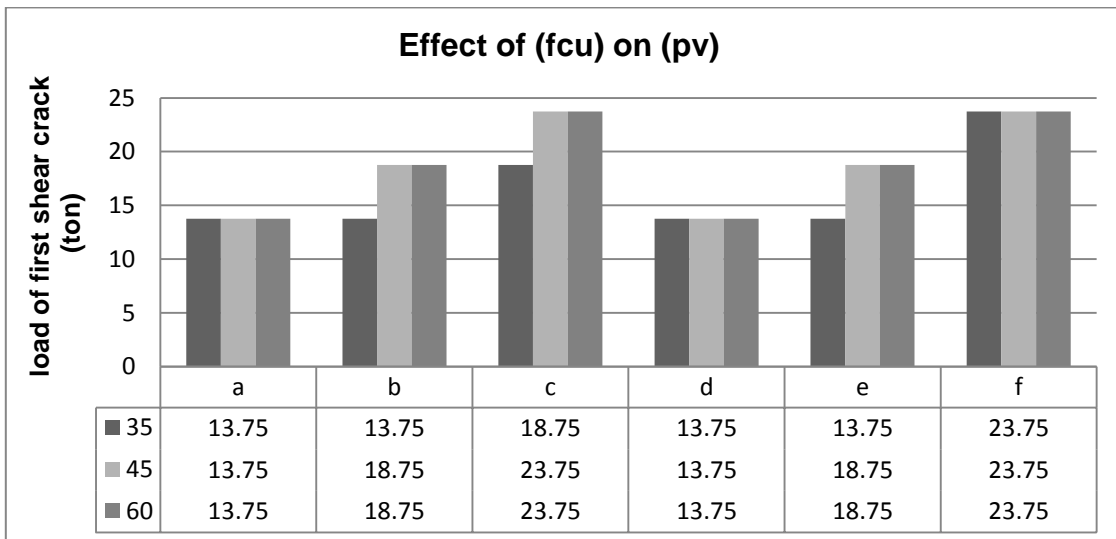
Figure 11: Effect of characteristic strength (f_{cu}) on load of first shear cracks (p_v)
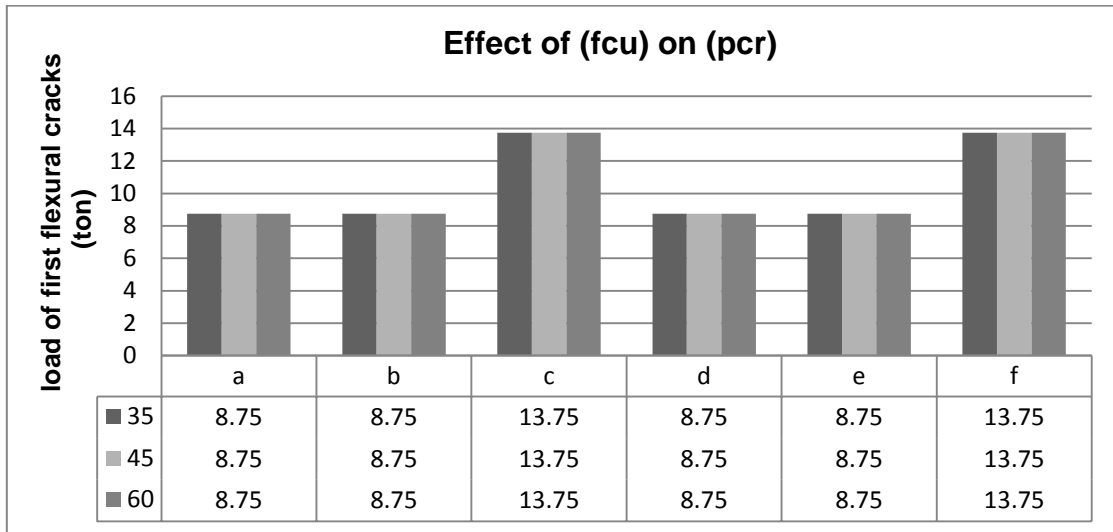
Figure 12: Effect of characteristic strength (f_{cu}) on load of first flexural cracks (p_{cr})
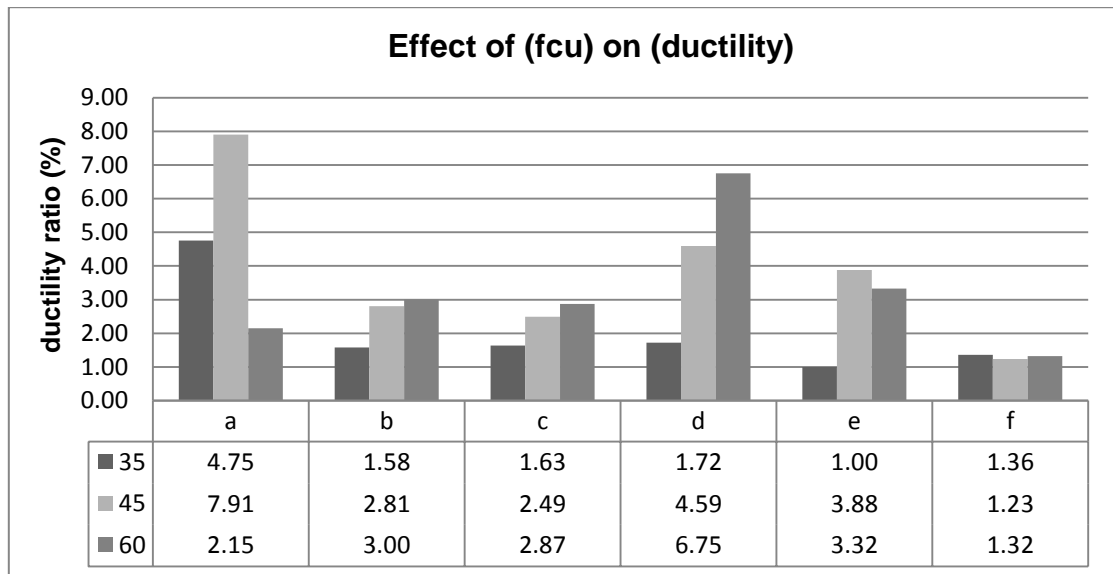
Figure 13: Effect of characteristic strength (fcu) on ductility ratio (%).

Effect of stiffness ratio between column and wall (tc/tw) on ultimate horizontal load capacity, load of first shear cracks, load of first flexural cracks, and ductility can be demonstrated by figures 14, 15, 16, and 17 respectively. Samples are assembled through a table beneath every single bar-chart according to table (6).

Table (6) Samples assembly for the case of effect (t_c/t_w)

	a	b	c	d	e	f	g	h	j
group (1)	1	2	3	7	8	9	13	14	15
group (2)	4	5	6	10	11	12	16	17	18

Effect of (tc/tw) on (pu)

	a	b	c	d	e	f	g	h	j
group one	25	30	48.75	26.88	38.75	58.75	23.75	43.75	63.75
group two	18.75	23.75	61.25	26.25	43.75	65	33.75	41.25	83.75

ultimate horizontal load (ton) — vertical axis
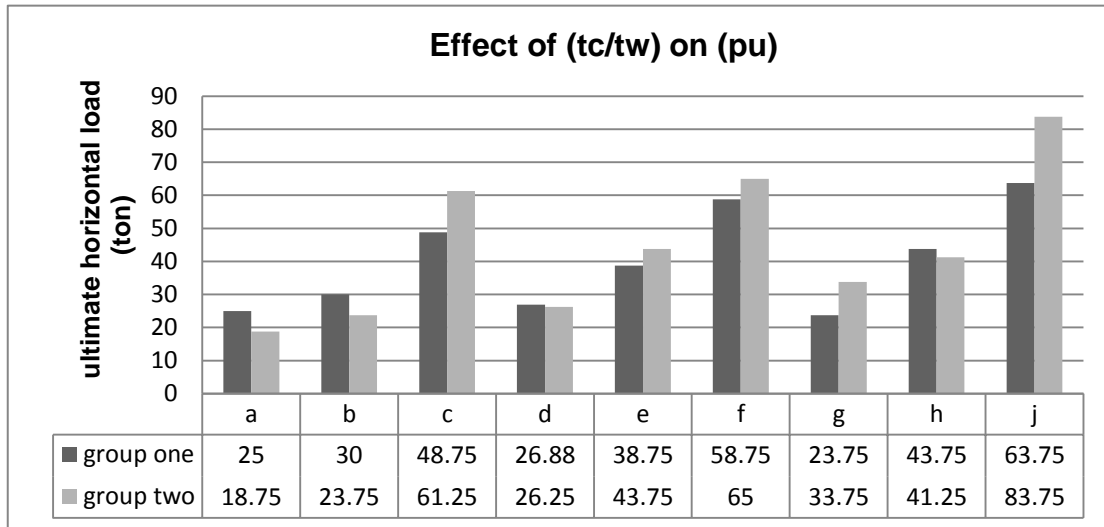
Figure 14: Effect of stiffness ratio (t_c/t_w) on ultimate horizontal load (p_u)

Effect of (tc/tw) on (pv)

	a	b	c	d	e	f	g	h	j
group one	13.75	13.75	18.75	13.75	18.75	23.75	13.75	18.75	23.75
group two	13.75	13.75	23.75	13.75	18.75	23.75	13.75	18.75	23.75

load of first shear crack (ton) — vertical axis
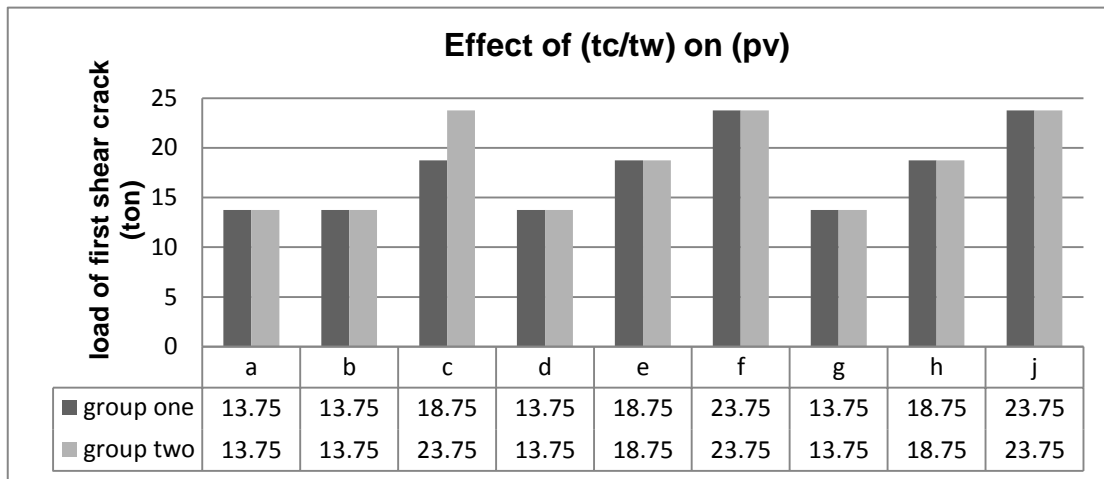
Figure 15: Effect of stiffness ratio (t_c/t_w) on load of first shear cracks (p_v)

Effect of (tc/tw) on (pcr)

	a	b	c	d	e	f	g	h	j
group one	8.75	8.75	13.75	8.75	8.75	13.75	8.75	8.75	13.75
group two	8.75	8.75	13.75	8.75	8.75	13.75	8.75	8.75	13.75

load of first flexural crack (ton) — vertical axis
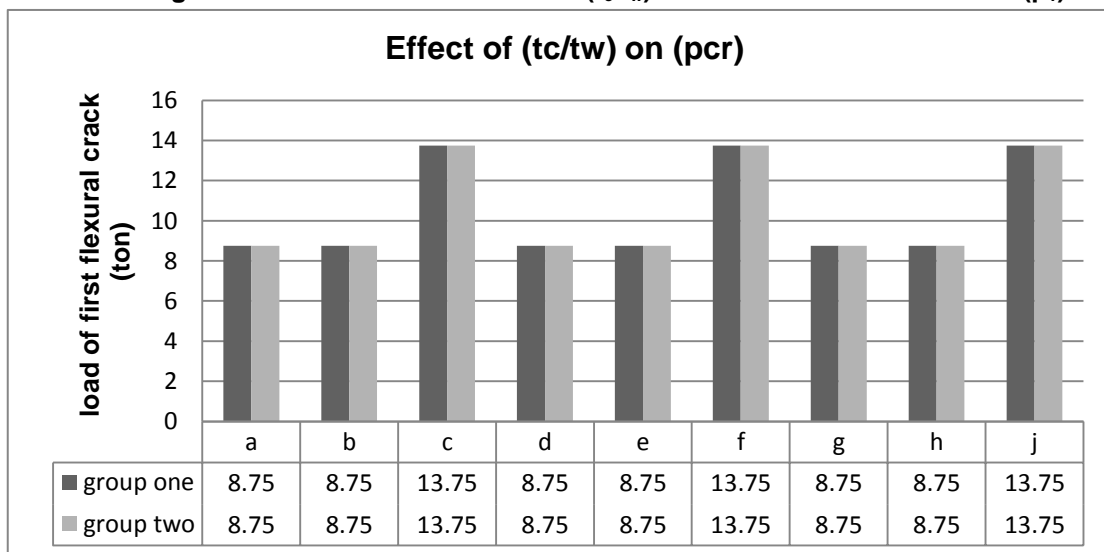
Figure 16: Effect of stiffness ratio (tc/tw) on load of first flexural cracks (pcr)

Effect of (tc/tw) on (ductility)

	a	b	c	d	e	f	g	h	j
group one	4.75	1.58	1.63	7.91	2.81	2.49	2.15	3.00	2.87
group two	1.72	1.00	1.36	4.59	3.88	1.23	6.75	3.32	1.32
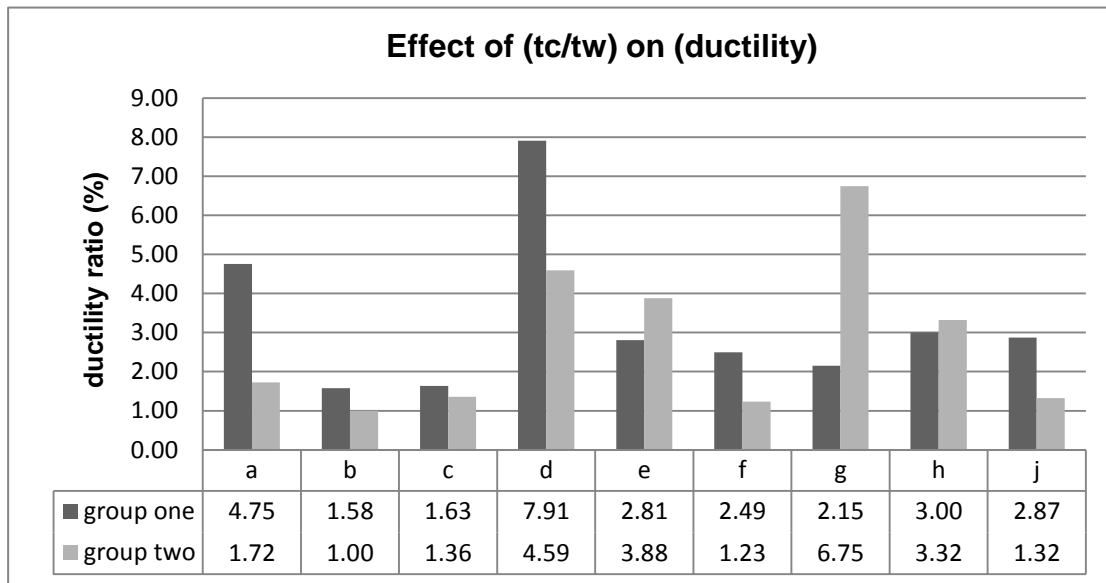
ductility ratio (%)

Figure 17: Effect of stiffness ratio (t_c/t_w) on ductility ratio (%).

CONCLUSION

According to the results obtained from the present non-linear analysis of coupled shear walls supported on two columns, the following conclusions may be drawn:

1- Ultimate horizontal load capacity is directly proportional to characteristic strength (f_{cu}). Increasing the characteristic strength (f_{cu}) from 35 to 45 MPa, and from 45 to 60 MPa, would lead to an increase in ultimate horizontal load capacity by nearly 25%, 11.68%, respectively. However, the ultimate horizontal load capacity would climb by about 10.61%, if the stiffness ratio went up from 37.5% to 51.25%.

2- First shear cracks are occurred mainly in transfer beam as well as connecting beams. If the characteristic strength (f_{cu}) climbed from 35 to 45 MPa, load of first shear cracks would go up by about 32.43%, whereas, increasing the characteristic strength (f_{cu}) from 45 to 60 MPa would not affect significantly on the position of first shear cracks. On the other hand, the position of first shear cracks does not be affected enormously by the variation in the stiffness ratio between column and wall.

3- Increasing or decreasing the characteristic strength (f_{cu}) and the stiffness ratio (tc/tw) would not affect significantly on the position of first flexural cracks. The position of these cracks mainly occurred in transfer beam. Load of first flexural cracks is direct proportion with characteristic strength (f_{cu}) and the stiffness ratio (tc/tw) but with a slight rate of increase.

4- Ductility of the whole system is direct proportion with characteristic strength (f_{cu}). Rising the characteristic strength (f_{cu}) from 35 to 45 MPa, and from 45 to 60 MPa, would lead to an increase in ductility by nearly 91%, 15%, respectively. Conversely, Ductility of the whole system would decrease to 13.89%, if the stiffness ratio (tc/tw) climbed from 37.5% to 51.25%.

5- The stiffness ratio between shear walls and supporting columns, under the effect of the lateral loads, is more crucial rather than characteristic strength and the reinforcement ratio.

REFERENCES

1. Morgan, A.S., 1992, "Linear and Nonlinear Analysis of Coupled Shear Walls Supported on Columns", M. Sc., Thesis, Structural Engineering Department, Faculty of Engineering, Cairo University, 222 pp.
2. Khaled, A.A., 2004, "Nonlinearity of Coupled R.C. Systems Part I: Coupled Shear Walls Supported on Columns", M. Sc., Thesis, Structure Engineering Department, Faculty of Engineering, Tanta University.
3. ANSYS user's manuals, April 2009, "Structural Analysis Guide", Release 12.0, ANSYS Inc. South pointe 275 Technology Drive Canonsburg, PA 15317.
4. Egyptian Code of Practice, 2007, ECP-203, "Design and Construction of Reinforced Concrete Structure", Ministry of Building Construction.
5. ACI Committee 318-14, 2014, "Building Code Requirements for Reinforced Concrete", American Concrete Institute, Farmington Hill, Michigan.
6. H. J. Pam, A. K. H. Kwan and M. S. Islam, November 2001, "Proceedings of the Institution of Civil Engineers", "Structures and Buildings 146", Issue 4, Pages 381-389.
7. Martinez, S., Nilson, AH. , And Slate, F.O., Aug. 1982, "Spirally-Reinforced High-Strength Concrete Columns", Research Report No. 82-10, Department of Structural Engineering, Cornell University, Ithaca.
8. K.J. Willam, and E. P. Warnke, 1974 ,"Constitutive Model for Tri-axial Behavior of Concrete", Seminar on Concrete Structures Subjected to Tri-axial Stresses, International Association of Bridge and Structural Engineering Conference, Bergamo, Italy.
9. James K. Wight, James G. Macgregor., 2011, "Reinforced Concrete Mechanics and Design", Sixth Edition.
10. Tavarez, F.A., 2001, "Simulation of Behavior of Composite Grid Reinforced Concrete Beams Using Explicit Finite Element Methods", Master's Thesis, University of Wisconsin-Madison, Madison, Wisconsin.
11. Coull, A., 1982, "Simplified Elasto-Plastic Analysis of Coupled Shear Walls", Proc. Instu. Civ., Part 2, 73, June, 365-381.
12. Timoshenko,S., Goodier,J.N., 1933, "theory of elasticity", First Edition, University of Michigan.
13. Salonikios, T. N., No. 6, June 2007, "Analytical Prediction of the Inelastic Response of RC Walls with Low Aspect Ratio", Journal of Structural Engineering, Vol. 133, pp. 844-854.
14. EL-Fadeel, A. A., 2017, "Non-linear Analysis of Single Coupled Shear Walls Supported on Columns", M.Sc., Thesis, Structural Engineering Department, Faculty of Engineering, Cairo university.
15. Zhou, J., 2003, "Effect of Inclined Reinforcement on the Seismic Response of Coupling Beams", M. Eng. Thesis, McGill University, Montreal.

APPENDIX A:

CALCULATIONS OF VERTICAL AND HORIZONTAL LOADS USING EGYPTIAN CODE OF PRACTICE "ECP- 203"

1. CALCULATIONS OF VERTICAL LOADS

The assumed data as the following:

- Live load = 400 kg/m^2
- Superimposed dead load = 150 kg/ m^2
- Wall bricks weight per square meter = 150 kg/ m^2
- Thickness of each slab = 220 mm

Factored vertical loads are calculated due to the weight of shear walls, coupling beams, columns, in addition to loads from the weight of slabs, as shown in the following equation:

•Total vertical factored load = 1.4(weight of shear walls+ coupling beams+ columns) + 9× area of slab within the wall zone× weight of slab.

•Total vertical factored load = 1.4((2.5×4×25.5×0.5×2) + (4×0.5×0.6×2.5×10) + (2×0.5×1.5×4×2.5)) + 9×45.6× (1.4× (0.22×2.5+0.15) +1.6×0.4) =1084.85 ton.

•Concentrated vertical loads/story = 1084.85/9 =120.54 ton.

•Distributed vertical loads/story =120.54/12 =10.045 t/m =100 kN/m.

2. CALCULATIONS OF HORIZONTAL LOADS

Horizontal loads which acting on the coupled system are calculated by the response spectrum analysis using ECP-203 [4], as shown in the following steps:

The assumed data as the following:

- Cairo-zone (3)
- Soil type (D)
- Total height above foundation= 29.5 m
- Important building

The total design seismic base shear (Fb) along any principal direction is given by the following equation:

$$\bullet \, Fb = Sd(\text{Ti}) \times \lambda \times \frac{\text{w}}{\text{g}}$$

Where,

W = Seismic weight of the whole building, is sum of the seismic weight of all floors.
$Sd(\text{Ti})$ = Design horizontal acceleration spectrum value which is determined by using the following expression:

$$\bullet \, Sd(\text{Ti}) = \text{ag} \times \gamma 1 \times \text{S} \times \frac{2.5}{\text{R}} \times \frac{\text{TC}}{\text{T1}} \times \xi \qquad \text{In case of} \qquad \text{Tc} \le \text{Ti} \le \text{T}_\text{D}$$

In Which,
- T1 = The fundamental period of vibration of the building in the direction of analysis;
- ag = The design ground acceleration;
- R = Response modification (Force Reduction) Factor as a ratio between the elastic and plastic internal forces in the building, illustrated in Code Table (8.A);

- $TC, TB, TD,$ and S = illustrated in Code Table (8.3);
- ξ and $\gamma1$ = illustrated in Code Tables (8.3) and (A.4)

3. CALCULATIONS OF FINAL FORCES ON EACH FLOOR LEVEL:

- Soil class D, (S=1.8, T_b=0.1, T_c=0.3, T_D=1.2, ag= 0.159, Ct=0.05).
- $Ti = Ct\, H^{3/4} = 0.05 \times (29.5^{\frac{3}{4}}) = 0.633 < 4\, Tc = 1.2$
- $Tc \le Ti \le T_D$
- (ξ=1.0, $\gamma1$=1.4, R= 5)
- ag= 0.15× 9.81 =1.4715 m/sec^2
- $Sd(\text{Ti}) = ag \times \gamma1 \times S \times \frac{2.5}{R} \times \frac{TC}{T1} \times \xi$
- $Sd(\text{Ti}) = 1.475 \times 1.4 \times 1.8 \times \frac{2.5}{5} \times \frac{0.3}{0.633} \times 1.0 = 0.879$
- $Fb = Sd(\text{Ti}) \times \lambda \times \frac{w}{g}$
- Wt. of floors = (20×30× (0.22×2.5+0.15+0.15)) ×9 =4590 ton
- Wt. of shear walls, columns = 2×2.5× (0.5×4) ×29.5 =295 ton
- $W_{D.L}$ = 295+4590 = 4885 ton
- $W_{L.L}$ = 9×0.4×20×30 =2160 ton
- $W_{D.L}$+0.5× $W_{L.L}$ =5965 ton
- $Fb = 0.879 \times 1 \times \frac{5965}{9.81} = 534.48$ ton
- W_i = 5965 /9 = 662.78 ton/floor
- $\sum W_i\, H_i$ = 662.78 (5.5+8.5+11.5+14.5+17.5+20.5+23.5+26.5+29.5) = 104387.85 t.m
- $Fi = \frac{Wi\, Hi}{\sum Wi\, Hi} \times Fb$
- $Fi = \frac{662.78 \times 534.48}{104387.85} \times Hi$
- $Fi = 3.39 \times Hi$

- The final horizontal and vertical loads can be illustrated as shown in figure (A.1).
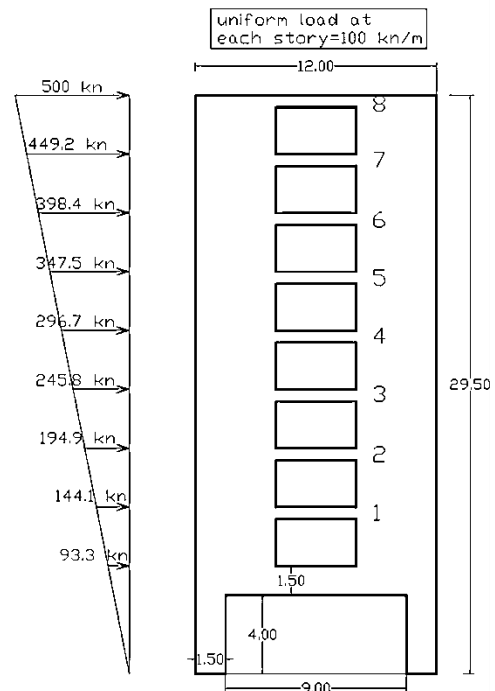
Figure A.1: Final vertical and horizontal loads acting on the coupled system.